A Microscopic Description of Concentrated Potassium Fluoride Aqueous Solutions by Molecular Dynamics Simulation

Yann Laudernet,[†] Thierry Cartailler,*[,†] Pierre Turq,[†] and Mauro Ferrario[‡]

Laboratoire Liquides Ioniques et Interfaces Chargée, Université Pierre et Marie Curie, 4 place Jussieu, 75252 Paris CEDEX 05, France, and INFM and Dipartimento di Fisica, Università degli Studi di Modena e Reggio Emilia, Via G. Campi 213/A, 41100 Modena, Italy

Received: November 7, 2002

We describe the microscopic structure and dynamical properties of potassium fluoride aqueous solutions at $T = 298$ K as a function of concentration up to 11.9 M. All calculations are made using constant temperature and pressure as well as microcanonical molecular dynamics simulations on the basis of an optimized pair potential model which is a mix of Coulomb plus standard Lennard-Jones short-range terms for water and ion−water interactions and Tosi-Fumi potential for ion−ion interactions. In particular we propose a modified ion−water interaction that successfully reproduces the experimental behavior of the density and water self-diffusion of the solutions as a function of concentration. Finally, we analyze hydrogen-bonding in solutions looking at pair distribution energies and residence times. We find strong evidence for K^+-F^- pairing in solutions at the higher concentrations.

I. Introduction

In comparison with the huge number of experimental and simulation studies where water in the liquid and glassy states has been the center of interest, only a few calculations exist for highly concentrated ionic solutions. Furthermore, almost all simulations of electrolyte solutions focus on systems composed by only one ion, or at most a pair of ions, in a relatively large number of solvent molecules,[1−14] while results of integral theories obtained in the infinite dilution limit are used to compare calculated mobilities, limit conductivities, and friction coefficients.[3,7,11] Historically, for pure solvents, and in particular for water, several potential models have been proposed to be used in simulations and also a number of comparative studies have been published.[15−17] More recently, a few models have been established, starting from ab initio calculations, which successfully reproduce various physical conditions. On the other side, models for ion−ion interactions also have a very long history. Effective Huggins-Mayer pair interaction potentials, parametrized to reproduce the ionic crystal phase, were proposed by Tosi and Fumi[18,19] and successfully used also to reproduce accurately the physical properties of molten salts.[20,21] For ion−water interactions, only a few pair interaction models are available. Mostly they were obtained from ab initio calculations of clusters composed of a single ion surrounded by a few water molecules[4,10,22] and tuned to reproduce physical properties in the so-called "infinitely diluted conditions". Each of these models is tuned with a particular solvent model, with respect to which ab initio data were optimized, so that different sets of parameters are listed for different solvent models.[7,9] As it has been noticed,[2,13] the parameters from these single ion−solvent interactions cannot be generalized using standard mixing rules for simulations where many ionic species are present in the cell, and in particular they tend to give very poor results for the solid phases compared to the Tosi-Fumi ones.

Some of the most used parameters for ion−water interactions are those of Dang and Smith.[9] NaCl aqueous solutions were studied using these parameters by molecular dynamics simulations[8] in the range of concentration from 0.55 up to 4.1 mol/L, corresponding to a number of ion pairs in the MD box ranging from 5 to 20. For both structural and dynamical properties, the comparison between simulation and experimental data is far from being satisfactory.

Although several other simulation studies of NaCl solutions were performed,[5,23−25] little exists for other alkali halides, in particular for the fluoride ion, which has the interesting property of making strong hydrogen-bonds with the hydrogen atoms of water. In the present work we analyze the structural and dynamical properties of concentrated KF aqueous solutions by MD simulations. We made a first calculation by using a composite model with parameters fully taken from the literature: SPC/E model for water−water interactions,[26,27] Dang-Smith potential parameters for the ion−water interactions,[28,29] and Tosi-Fumi potential model for ion−ion interactions.[18,19] This model was inadequate to reproduce consistently simple physical properties as a function of solute concentration. To overcome this problem we propose here a new model which keeps the same functional structure with adjusted parameters for ion−water interaction. The outline of this article is as follows: in Section 2 we give details on the pair interaction potential models and conditions we used in our simulations; in Section 3 we show results for some fundamental property of the solutions obtained by both potentials with comparison to experimental data; finally, we describe structural and dynamical properties, respectively, in Section 4 and Section 5, obtained with the adjusted potential model for KF aqueous solutions up to very high concentrations.

II. Interaction Potentials and Simulation Details

For modeling aqueous solutions of potassium fluoride we adopt a potential model with the simplest possible structure. The rationale for such a simplified choice lies in the fact that we want to use such a model for very extensive (and expensive)

* Corresponding author. Fax: 33 144273834. E-mail: cartail@ccr.jussieu.fr.
[†] Université Pierre et Marie Curie.
[‡] Università degli Studi di Modena e Reggio Emilia.

10.1021/jp0223814 CCC: $25.00
Published on Web 02/19/2003

TABLE 1: Potential Parameters for Tosi-Fumi Model for Potassium Fluoride

ion−ion	A (kJ/mol)	ρ (Å)	C (kJ/mol/Å^6)	D (kJ/mol/Å^8)
K−K	146455.0	0.338	1463.3	1445.3
K−F	50562.9	0.338	1174.3	1264.6
F−F	16365.6	0.338	1120.1	1324.8

free energy calculations of concentrated electrolyte solutions, and with the present study we try to validate the model by exploring standard structural and dynamical properties of these solutions. Water molecules are considered rigid and interactions are modeled as a sum of pair contributions, composed of an electrostatic term and a van der Waals term which is represented by a standard Lennard-Jones potential for water−water and ion−water while for ion−ion interactions the full Tosi-Fumi structure is used with the r^{-8} term also included. The electrostatic term is modeled by using fixed partial charges with the elementary interaction given as usual by

$$V_{ij}^{c}(r_{ij}) = \frac{e^2}{(4\pi\epsilon_0)}\frac{Z_i Z_j}{r_{ij}} \tag{1}$$

where Z_i is the atomic valence, e the elementary charge, ϵ_0 is the vacuum permittivity, and r_{ij} is the site−site distance. Long-range contributions are included by means of a standard Ewald summation procedure. As described before, the functional form of short-range terms varies depending on the different model used to describe site−site interactions. For water−water interactions we have used the SPC/E model[26,27] which may be one of the best nonpolarizable pair potentials to describe pure solvent properties.[17] Molecular geometries are fixed, the intramolecular O−H distance is 1 Å, and the $\widehat{HOH}$ angle is 109.47°. Partial charges on each atom (0.4238e for hydrogen atoms and −0.8476e for oxygen atoms) are also fixed and, finally, to describe short-range interactions this potential uses a classical Lennard-Jones 12-6 term between oxygen atoms, with hydrogen ones being considered as fully enclosed in the oxygen sphere.

$$V_{ij}^{\mathrm{LJ}}(r_{ij}) = 4\epsilon_{ij}\left[\left(\frac{\sigma_{ij}}{r_{ij}}\right)^{12} - \left(\frac{\sigma_{ij}}{r_{ij}}\right)^{6}\right] \tag{2}$$

with $\epsilon_{OO} = 0.652$ kJ/mol and $\sigma_{OO} = 3.166$ Å.

We chose the Tosi-Fumi potential[18,19] for ion−ion interactions, expressed as

$$V_{ij}^{\mathrm{TF}}(r_{ij}) = A_{ij}e^{-r_{ij}/\rho_{ij}} - \frac{C_{ij}}{r_{ij}^{6}} - \frac{D_{ij}}{r_{ij}^{8}} \tag{3}$$

where the four parameters A_{ij}, ρ_{ij}, C_{ij}, and D_{ij} are given in Table 1 with charges fixed to the ion values. The choice of the parameters for the ion−water interaction is crucial in order to determine the properties of highly concentrated aqueous solutions. Electrostatic interactions are already fixed, defined by the choices of the interactions for like pairs. As anticipated in the Introduction, we have initially taken literature values from Dang for the parameters of the ion−water Lennard-Jones interaction The parameters are $\epsilon_{KO} = 0.5216$ kJ/mol and $\epsilon_{FO} = 0.699$ kJ/mol,[28] $\sigma_{KO} = 3.250$ Å and $\sigma_{FO} = 3.143$ Å,[29] respectively.

We shall refer to the above-described model potential, with all parameters taken from the literature as Potential 1, to distinguish it from the modified model, Potential 2, which differs from the first by the value of a single parameter, the distance σ_{FO} which has been moved up to 3.220 Å in order to achieve a behavior with concentration more representative of the experimental data for some basic physical properties of the solution. More details will be presented in the next section. Although the change may appear to be a minor one, it has to be noted that changing the size of the repulsion core of the fluoride ion has a strong influence on the balance of the electrostatic interactions, modifying in a substantial way the energetics of water−fluoride hydrogen-bonding, with consequent relevant changes not only on the densities but also in the dynamical properties of the solution. Other, more extensive modifications of the potential parameters have also been tried, but we report here only the one that gave the best agreement with experimental results.

TABLE 2: Number of Water Molecules, N_W, and Number of KF Pairs, N_{KF}, for Each Simulated System at Different Concentration and Related Molality (number of moles of solute/kg of water)

system	1	2	3	4	5	6	water
N_W	680	960	640	384	451	494	256
N_{KF}	35	64	64	64	87	128	0
molality	2.84	3.70	5.56	9.26	10.72	14.40	0

Simulations have been carried out at constant temperature and pressure using cubic boxes with periodic boundary conditions[30] for structural determination. Short-range interactions have been evaluated with a spherical cutoff radius as close as possible to the half MD box length. As already mentioned, the long-range character of electrostatic interaction has been taken care of by using Ewald summations[31] to calculate energies and forces. For all simulations we used the same values for the dimensionless convergence parameter $\alpha L = 5.6$, where L is the size of the cubic box. The number of k vectors has been adjusted to achieve a sufficient degree of convergence in the calculation of energies and forces. The numbers of water molecules and KF ion pairs used at each concentration are listed in Table 2 as a function of the molality of the solutions. For convenience we have labeled the different solutions with numbers going from 1 to 6 with increasing concentration and will make reference to these labels in the text. Water molecules have been kept rigid, i.e., by integrating the equations of motion by means of the generalized method of constraints.[32−34]

For all concentrations we worked at a fixed thermodynamic point with $T = 298$ K and $P = 1$ bar. The time step was the same for all solutions, $\Delta t = 2.5$ fs, while a slightly smaller one, $\Delta t = 1.5$ fs, was used for consistency checks in some runs with pure water. The equilibration of each system consisted of at least 40 000 time steps at constant volume, initially in the microcanonical (NVE) but mostly in the canonical (NVT) ensemble. Successively, a similar length of time was used to equilibrate the system in isothermal−isobaric conditions (NPT). Production runs of 100 000 time steps have accumulated, and have been used to calculate structural and thermodynamics averages. Calculations in the (NVT) ensemble were done using the Nosé-Hoover[35−38] approach. For the (NPT) ensemble, we use a generalization of the Andersen constant pressure method[39,40] with coupling of the pressure bath to the molecular center of mass degrees of freedom. After calculating densities as averages from the (NPT) trajectories, the corresponding values for the volume were used to generate standard microcanonical trajectories of similar length, since in simulation in the NPT ensemble dynamical properties can be severely affected in a nonphysical way. From these microcanonical simulations we calculated the dynamical properties of our systems, in particular the time correlation functions needed to estimate self-diffusion coefficients and residence times of water molecules around ions.

TABLE 3: Aqueous KF Solution Concentrations (C_{KF} in mol/L) and Densities (ρ in g/cm^3) Calculated with Potential 1 (Pot 1) and Potential 2 (Pot 2) Compared to Experimental Values (expt)

	1		2		3		4		5		6	
system	C_{KF}	ρ	C_{KF}	ρ	C_{KF}	ρ	C_{KF}	ρ	C_{KF}	ρ	C_{KF}	ρ
(expt)	2.76	1.12	3.53	1.16	5.14	1.22	8.06	1.34	9.09	1.38		
(Pot 1)	2.84	1.16	3.66	1.20	5.37	1.28	8.41	1.40	9.45	1.43	11.88	1.52
(Pot 2)	2.77	1.13	3.55	1.16	5.16	1.23	8.09	1.34	9.09	1.38	11.32	1.44

TABLE 4: Partitions of Average Potential Energies Calculated with Potential 1 (Pot 1) and the Potential 2 (Pot 2) as a Function of Molality: (total) Average Total Potential Energy, (W−W) Contribution from Water−Water Interactions, (W−K$^+$) Contribution from Water−Potassium Ion Interactions, (W−F$^-$) Contribution from Water−Fluorine Ion Interactions, (E−E) Contribution from Electrolyte−Electrolyte Interactions

	1		2		3		4		5		6	
system	Pot 1	Pot 2	Pot 1	Pot 2	Pot 1	Pot 2	Pot 1	Pot 2	Pot 1	Pot 2	Pot 1	Pot 2
total	−87.0	−85.1	−98.1	−95.6	−121.5	−117.8	−164.4	−158.5	−179.0	−173.9	−213.6	−207.2
W−W	−25.1	−32.0	−20.7	−29.6	−13.8	−24.3	+0.5	−17.3	+1.6	−15.1	+3.1	−9.7
W−K$^+$	−12.2	−6.13	−13.8	−5.5	−15.2	−8.9	−20.5	−7.1	−19.6	−7.1	−17.8	−10.0
W−F$^-$	−31.4	−21.4	−38.5	−25.8	−50.2	−31.1	−72.7	−43.9	−73.8	−46.4	−75.3	−51.3
E−E	−18.3	−25.5	−25.1	−34.6	−42.1	−53.3	−71.5	−90.1	−87.0	−104.2	−123.5	−136.1

[a] All energies are expressed in kJ/mol where for the normalization we have considered as the number of molecules in each system the sum of the number of water molecules plus the number of ion pairs.

III. Comparison with Experimental Data

In this paragraph, we present the results of molecular dynamics calculations performed using both Potential 1 and Potential 2 and compare them with available experimental data for KF aqueous solutions for densities and water self-diffusion coefficients as a function of the salt concentration.

First we calculated densities for pure water and KF aqueous solutions as a function of salt concentration (C_{KF}) for both potential models, and compared them to experimental ones[41] in order to test the validity of both models. Results are summarized in Table 3 and graphically shown in Figure 1. All calculations were performed in the NPT ensemble in order to estimate the density of solutions predicted by both models. Since experimental values do not exist for concentration higher than 10.382 mol/L,[41] we extrapolated the values in this region by means of a standard numerical fitting procedure. All explored concentrations are below the limit of solubility which is close to 13.5 mol/L at our thermodynamic conditions.

The experimental value for the density of pure water at 298 K is equal to 0.99707 g/cm^3.[41] Our result of 0.99 ± 1% g/cm^3 offers a sufficiently good accuracy for a MD calculation, as it was expected, at these thermodynamic conditions, using the SPC/E model.

For the case of KF aqueous solutions, the estimated error on the calculations was again close to 1%. The comparison between Potential 1 and experimental data shows differences as large as 5%, with the calculated density being always higher than the experimental one for all concentrations, which suggests that this potential model is too hallows for too much attraction.

Potential 2 gives a difference smaller than 1% in comparison to experimental data, which shows how the increase in the repulsive core of the O−F interaction results overall in a less attractive behavior by decreasing the strength of the electrostatic water−fluoride attraction. This is confirmed by inspecting the way in which the potential energy partitions into single contributions. To this end, in Table 4 we report the average total potential energy for each system and its breakup into the two like contributions, for the interactions between the water molecules and for the interactions between the ions, and the two mixed contributions for the interactions of water molecules with the potassium and the fluorine ions. The major feature that one can observe is that Potential 2 favors the like-interactions giving less negative values with respect to Potential 1 for the configurational energies of water with both the fluorine ions (as expected) and the potassium ions, which at higher concentrations even displays a questionable positive configurational energy for the water−water interactions.

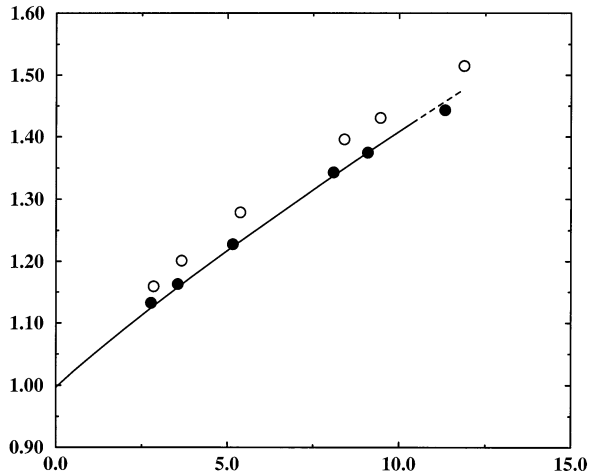

Figure 1. Density (g/cm^3) as a function of salt concentration (mol/L): experimental data (solid line) and extrapolated data (dashed line), calculations from Potential 1 (white circle) and Potential 2 (black circles).

Because the behavior of just one physical (structural) property cannot be a sufficient test to compare the relative performances of the two model potentials, we chose to associate it with the behavior of a dynamical property, the self-diffusion of water in the solution as a function of salt concentration.

We have calculated the self-diffusion coefficient D_W of water by mean of simulations in the NVE ensemble, as functions of salt molalities (m_{KF}) for both potentials, by using a linear fit to the long time behavior of Einstein's mean square displacements.

We compare here our results to experimental values[42] in Table 5. As it can be seen in Figure 2 , diffusion coefficients calculated with Potential 1 are very far from experimental values. At the highest concentrations, water diffusion is severely hindered, solutions seem to be practically frozen with water behaving more as in a gel than in a liquid. Again we trace such behavior to the too large attraction character of Potential 1. On the other hand, values calculated with Potential 2 are in good agreement with experimental ones at all molalities.

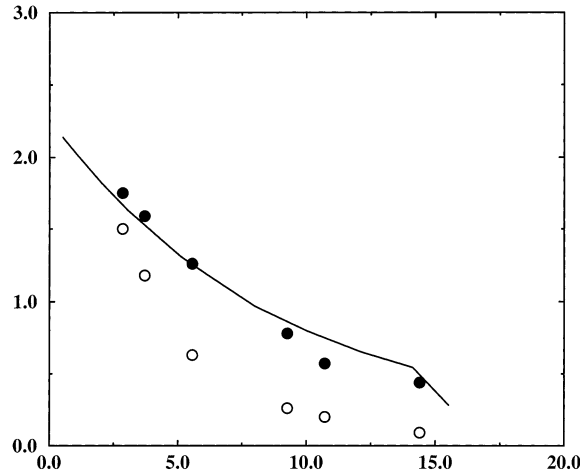

Figure 2. Self-diffusion coefficients of water (10^{-9} m^2/s) as a function of molality (number of moles of solute/kg of water): experimental data (solid line), and calculations from Potential 1 (white circle) and Potential 2 (black circles).

TABLE 5: Self-diffusion Coefficients D_W (10^{-9} m^2/s) of Water Molecules in Aqueous KF Solution Calculated with Potential 1 (Pot 1) and the Potential 2 (Pot 2) Compared to Experimental Values (Expt), as a Function of Molality

configuration	1	2	3	4	5	6
D_W (Expt)	1.65	1.52	1.25	0.85	0.74	0.48
D_W (Pot 1)	1.50	1.36	0.63	0.26	0.20	0.14
D_W (Pot 2)	1.70	1.59	1.26	0.78	0.57	0.41
molality	2.84	3.70	5.56	9.26	10.72	14.40

In the eyes of these results, we can conclude comfortably that the Potential 2 is the most appropriate to study KF aqueous solutions as a function of salt concentration.

IV. Structural Aspects

Our goal is now to study the microscopic structure of the concentrated solutions, to determine the ion solvation structure, to estimate the effects of the presence of ions on the structure of water, and to compare it with the pure water case. We have first of all calculated the intermolecular partial radial distribution functions, $g_{ij}(r)$, for each KF solutions. We show the various $g_{ij}(r)$ at four C_{KF} and pure water (with r in Å) in Figures 3−6. The errors in the positions of the $g_{ij}(r)$ are of ±0.05 Å, and of ±0.1 for the coordination numbers. The distances and angles discussed below were all calculated from system 4 (at C_{KF} = 5.16 mol/L), the $g_{ij}(r)$ related to this concentration always appears as a full line in the figures. The values given for Potential 1 in Table 6 and Figure 7 will be used in the Discussion section.

Let us consider first the solvation of the potassium ion (Figure 3). The solvation structure of K^+ is very well defined, with distinct peaks for both $g_{KO}(r)$ and $g_{KH}(r)$, centered at 2.82 and 3.36 Å, respectively. Estimating that both peaks are relative to a single water molecule, and assuming that the lonely $g_{KH}(r)$ peak implies that both hydrogens play the same role, we can calculate the angle θ between $\overrightarrow{KO}$ and the dipole vector of the water molecule. We find $\theta = 51 \pm 8°$, which is in good agreement with the experimental data available from neutron scattering of LiCl in water and with various simulations of a single potassium ion surrounded by water molecules (Table 6).

The positions of the first maxima do not change with salt concentration, but the structure around the potassium beyond the first hydration shell is notably modified. The first KH peak becomes wider as the salt concentration grows, and the following

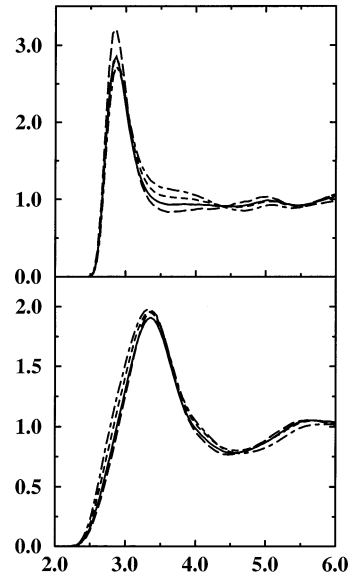

Figure 3. Partial distribution functions $g_{KO}(r)$ (up) and $g_{KH}(r)$ (down) at different concentrations: C_{KF} (mol/L) = 2.77 (long dashed line), 5.16 (solid line), 8.09 (dashed line), 11.32 (dot−dashed line), with axis unit in Å.

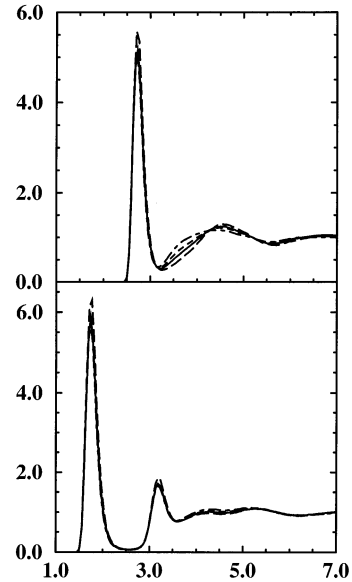

Figure 4. Partial distribution functions $g_{FO}(r)$ (up) and $g_{FH}(r)$ (down). Same symbols as in Figure 3.

minimum is shifted to higher distance values. A shoulder develops into a second KO peak around 3.6−3.9 Å, enclosed in the first one, becoming pronounced from 8.09 mol/L. This feature alters the usual concept of solvation shell, as the position of the first minimum, usually taken to define its extension, becomes unclear. As a result, coordination numbers may loose their usual meaning. Calculating them using the position of the first minimum of $g_{KO}(r)$ at the lowest concentration (i.e., for r_{KO} = 3.63 Å), we found a constant number of 6 except for the most concentrated solution where n_{KO} is close to 5. These results are smaller than those calculated in simulation of a single K^+ ion in water (Table 6).

We now consider the solvation structure of the fluoride ion (Figure 4). The sharp first FH peak is characteristic of hydrogen-bonding. As for the case of the potassium ion, taking the positions of the first FO and the first and second FH peak as indicative of the atoms of a single water molecule, we have calculated the angle φ, defined here as the angle between the

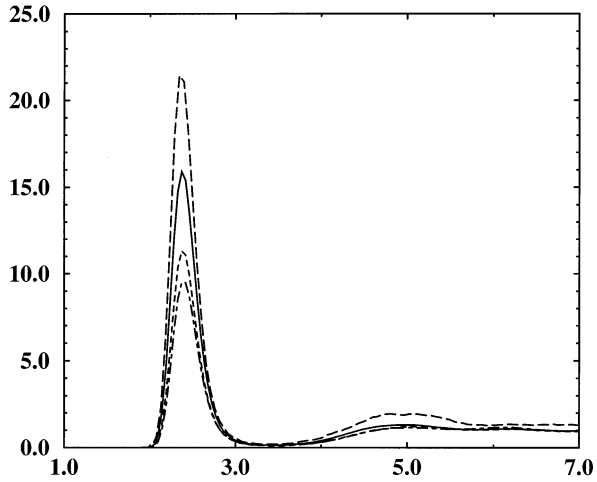

Figure 5. Partial distribution function $g_{KF}(r)$. Same symbols as in Figure 3.

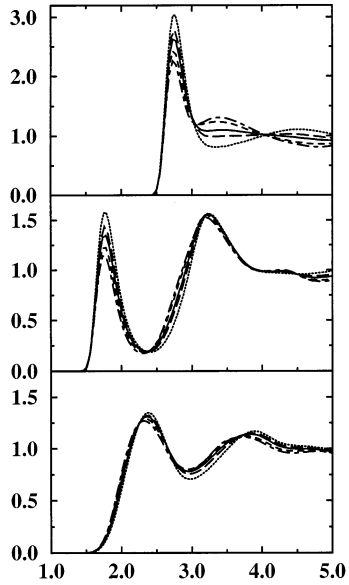

Figure 6. Partial distribution functions $g_{OO}(r)$ (up), $g_{OH}(r)$ (center), and $g_{HH}(r)$ (down) at C_{KF} (mol/L) = 2.77 (long dashed line), 5.16 (solid line), 8.09 (dashed line), 11.32 (dot−dashed line), and in pure water (dotted line), with axis unit in Å.

$\overrightarrow{FH}$ bond and the $\overrightarrow{OH}$ bond, and we found $\varphi = 170 \pm 8°$. While our calculated angle φ is consistent with other simulation results obtained for a single F^- in water (Table 6), our value for the FO distance is far greater, as we would have expected, due to the increased value of σ_{OF} in our Potential 2.

The positions of the first peak of the $g_{FO}(r)$ and both first and second peaks of the $g_{FH}(r)$ are practically unchanged with the salt concentration C_{KF}, while the second peak of g_{FO} is shifted to lower distances when the C_{KF} grows. Thus, in contrast to the potassium behavior, the first "hydration shell" of the fluoride ion is always well defined, but beyond it the solvation structure is difficult to read, especially for the most concentrated solutions. As for the potassium, our values for the coordination numbers are smaller than those reported in the other calculations (Table 6): 5 for the less concentrated solution going down to 3.5 for the highest.

The $g_{KF}(r)$ are shown in Figure 5. A sharp peak appears at 2.37 Å and decreases in magnitude with salt concentration. The relative coordination number goes from 1, at the lowest concentration, up to 2 at the highest. There are no contact pairs of ions with the same charge. The position of the first peak for the $g_{KK}(r)$ is at 4.05 Å, while for the $g_{FF}(r)$ the position of the first peak is at 4.36 Å. Both $g_{KK}(r)$ and $g_{FF}(r)$ do not change significantly with salt concentration C_{KF}.

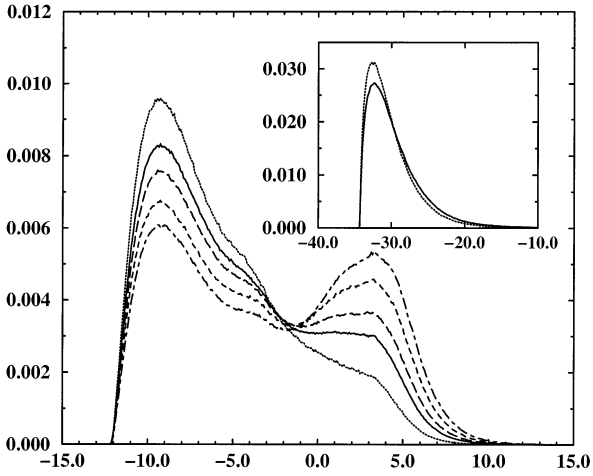

Figure 7. Probability distribution for the potential energy of water dimers in k_BT unit (same symbols as in Figure 6) and, encapsulated, for fluoride−water pairs at C_{KF} = 5.16 mol/L using Potential 2 (solid line) and Potential 1 (dotted line).

TABLE 6: Results of Our Simulations for Some Structural Parameters (as detailed in the text) at C_{KF} = 5.16 mol/L for Both Potentials Compared to Literature Values Obtained with Various Simulation Techniques and to the Values Measured by Neutron Scattering for a 3.57 Molal Aqueous LiCl Solution[a]

system	technique	model	r_{KO}(Å)	r_{KH}(Å)	n_{KO}(r)	θ	ref
$LiCl/H_2O$	expt					40	[52]
K^+/H_2O	MC	TIP4P	2.87	3.35	8.04	37−46	[53]
K^+/H_2O	MD	MCY	2.76	3.35	7.5	36	[3]
K^+/H_2O	MD	TIP4P	2.86	3.32	7.6	55	[4]
K^+/H_2O	MD	SPC/E	2.80		7.1		[11]
K^+/H_2O	QM/MM		2.81		8.3	60	[12]
K^+/H_2O	CPMD		2.81	3.44	6.75	56	[13]
KF/H_2O	MD	SPC/E	2.91	3.36	7.8	57	pot 1
KF/H_2O	MD	SPC/E	2.86	3.36	5.9	51	pot 2

system	technique	model	r_{FO}	r_{FH}	$n_{FH}(r)$	φ	ref
F^-/H_2O	MC	TIP4P	2.53	1.58	6.11	157(◇)	[53]
F^-/H_2O	MD	MCY	2.67	1.73	5.8	155(◇)	[3]
$F^-(H_2O)_4$	QM/MM	SPC(FQ)		1.76		174.2	[54]
F^-/H_2O	MD	SPC/E	2.60		6.3		[11]
KF/H_2O	MD	SPC/E	2.64	1.65	6.1	171	pot 1
KF/H_2O	MD	SPC/E	2.73	1.74	4.4	170	pot 2

[a] (◇) Angles calculated from distance values given in relative articles.

It is interesting to note that the number of first neighbors, n_K for K^+ ion and n_F for the F^- ion, defined by taking $n_K(r) = n_{KO}(r) + n_{KF}(r)$ and $n_F(r) = n_{FH}(r) + n_{KF}(r)$, remain nearly constant, with increasing C_{KF}. We find $n_K = 7.2-7.6$,while n_F goes from 6 down to 5.4. So the structure in the vicinity of both ions is characterized by the replacement of water molecules with the appropriate counterions with increasing C_{KF}.

Looking at the water−water structure, we find, as expected, a highly modified pattern of water because of the presence of numerous ions in comparison with the pure solvent case. The partial radial distribution functions $g_{ij}(r)$ for water pairs in solution are shown together with pure water ones in Figure 6. As for the fluoride solvation, the expected characteristic OH peak appears, indicative of a hydrogen-bond between two water molecules. Using the relative distances of each maxima, r_{OO} = 2.73 Å and r_{OH} = 1.76 Å, we have calculated the angle α (between $\overrightarrow{OH}_{intra}$ and $\overrightarrow{OO}$) and the angle β (between the dipole

moment of the "acceptor" water molecule and $\overrightarrow{OO}$) and found $\alpha = 11°$ and $\beta = 114°$, respectively. These values are in quite good agreement with the usual configuration of water dimers (at the quantum level, $\alpha = 5.5°$ and $\beta = 124.4°$[43]), and with the thresholds used in the usual hydrogen-bond geometric definitions (i.e., $r_{OO} \leq 3.5$ Å, and $\alpha \leq 30°$ [44−46]).

The effect of concentration is strong for both $g_{OO}(r)$ and $g_{OH}(r)$. The first peaks decrease with C_{KF}, and at longer distances the positions of the various maxima and minima appear to be reversed compared to pure water. The more striking change appears in the $g_{OO}(r)$. A second maximum which is not found in pure water becomes evident starting from the concentration value $C_{KF} = 5.16$ mol/L. As is in the case of the potassium ion, the minimum of the first OO peak cannot be clearly identified in contradiction with the usual "hydration shell" feature. It is known that the tetrahedral structure of water is characterized by a ratio close to 1.663 between the position of the two first maxima of $g_{OO}(r)$.[48] This is well confirmed in the case of pure water, where we find a value of 1.65, while in KF aqueous solutions the ratio goes to 1.57 at the lowest concentration and does not make much sense for higher concentrations. Thus, the $g_{OO}(r)$ clearly demonstrates that the structure of solutions is heavily disrupted by solvation, breaking the usual network pattern for hydrogen-bonding in water.

The first OH peak is usually considered as being characteristic of the existence of a hydrogen-bond between molecules. Here, his decline with C_{KF} implies a decreasing probability of having hydrogen-bonds between water molecules. But many articles point out the inadequacy of this simple criterion.[44,49] Thus we have calculated the probability distribution for the interaction energy of pairs of water molecules able to form a hydrogen-bond between them[48,50] (i.e., using a simple geometric criterion: $r_{OO} \leq 3.5$ Å, corresponding to the O−O distance criteria in the hydrogen-bond geometric definition in pure water). The result, as a function of C_{KF}, is plotted in Figure 7. Two peaks appear: the first is centered around $-9.4 \pm 0.08\ k_BT$, decreasing with C_{KF}; the second, which does not exist in pure water, is centered around $+3.1 \pm 0.08\ k_BT$, increasing with C_{KF}. The one at the negative value is clearly connected to hydrogen-bonding energies. We recover a linear hydrogen-bond geometry for a couple of water molecules at this energy.

We can now consider the energetic criterion for a hydrogen-bond, taken equal to $V_{H-bond} = -3.796\ k_BT$.[48] For Stillinger, this point corresponded to a true minimum of the curve. In our case, as for Ferrario et al.,[50] it corresponds to an inflection point, existing whatever C_{KF} is. This difference comes from the fact that Stillinger did not use a distance cutoff, including also water pairs which are not first-neighbor, but can as well have an attractive interaction energy. Stillinger et al. have also shown that this minimum does not depend on the temperature of the system, using the ST2 model for water.[47] This energetic point is then independent of both composition and temperature. Thus, for any pair interacting with an energy lower than V_{H-bond} we can consider that a hydrogen-bond exists. We are thus able to calculate the number of hydrogen-bonds (n_{H-bond}) between water molecules at each concentration (or molality), and compare to the water−water coordination number n_{OO} at $r_{OO} = 3.5$ Å (Table 7). The percentages of hydrogen-bonds are given ±1.5%, and the corresponding error for the number of hydrogen-bonds is ±0.4.

For pure water $n_{OO} = 4.8$, and we find $n_{H-bond} = 3.39$. This number is quite low, compared to other models,[15] and to the number of 4 expected to assume a perfect tetrahedral structure of water.

TABLE 7: Coordination Numbers for Water Oxygens (n_{OO}), Percentages of Hydrogen-Bond ($\%_{H-bond}$), and Average Numbers of Hydrogen-Bond per Water Molecule (n_{H-bond}) in Pure Water and as a Function of Molality in Aqueous KF Solutions

system	water	1	2	3	4	5	6
molality	0.00	2.84	3.70	5.56	9.26	10.72	14.40
n_{OO}	4.81	4.29	4.25	4.19	3.90	3.70	3.42
$\%_{H-bond}$	70.5	62,4	60.8	57.6	51.2	49.1	46.1
n_{H-bond}	3.39	2.68	2.58	2.41	2.00	1.82	1.58

TABLE 8: Self-Diffusion Coefficients $D_X(10^{-9}$ m^2/s) as a Function of Molality of Ions and Water in Aqueous KF Solutions Calculated with Potential 2

configuration	1	2	3	4	5	6
molality	2.84	3.70	5.56	9.26	10.72	14.40
D_K	0.89	0.67	0.52	0.30	0.23	0.18
D_F	0.72	0.65	0.49	0.28	0.24	0.17

When C_{KF} grows, n_{OO} and the percentage of hydrogen-bonds decreases, down to only 1.5 hydrogen-bonds at the highest concentration. But even so, at this concentration the percentage of hydrogen-bonds is equal to 46%. It implies that even with a large presence of ions in solution, many water molecules are still hydrogen-bonded, however the tetrahedral structure of water is lost.

Thus we have a double effect with increasing salt concentration on the pattern of water: the probability of finding hydrogen-bonds between two water molecules decreases with C_{KF}, and we can find pairs of neighboring water molecules, enclosed in ion solvation shells, that are constrained in an unfavorable configuration with a repulsive pair energy between them.

As a comparison, we have also calculated the pair energies between the fluoride anion and water molecules (boxed curve in Figure 7). The cutoff distance has been taken once more equal to the position of the first $g_{OF}(r)$ minimum, i.e., for $r_{OF} \leq 3.2$ Å. There is only one peak at negative energies, with the maximum of probability at $-32.3\ k_BT$, which represents for each C_{KF} 99% of all pairs. Thus, all the fluoride ions are hydrogen-bonded to their neighboring water molecules, with a binding energy far greater than the pair energy between hydrogen-bonded water molecules. This effect reinforces the idea of a solvation structure of the solution, which replaces the usual pattern of the hydrogen-bond network in water.

V. Dynamical Aspects

The calculated diffusion coefficients for K^+ and F^- ions, D_K and D_F, are given in Table 8. Our values are, as expected because of the highest densities, lower than those calculated in the infinite dilution limit ($D_K = 2.02$ and $D_F = 1.30 \times 10^{-9}$ m^2/s [9]). Starting from system 2 at concentration equal to 3.70 molal (i.e., 3.55 mol/L) up to the most concentrated solution, it can be seen that the self-diffusion coefficients of both ions are always very close. This may confirm the existence of long-leaving KF pairs in solutions, as it was already shown in the study of the ion solvation structure.

To investigate the stability of the various solvation shells of both ions, we have calculated the residence times of water molecules around them for all concentrations (Table 9). We follow the definition of the residence time given by Impey et al.[3] First, we define the characteristic distance r_{cut} between an ion and a water molecule under which the ion is supposed to be solvated by the water molecule. For each ion X, we have taken r_{cut} equal to the distance of the first minimum of the corresponding $g_{XO}(r)$. But in the case of K^+, we have also taken the distance of the minimum of the $g_{KO}(r)$ at the lowest C_{KF}, in

TABLE 9: Residence Times (ps), for a 204 ps Correlation Time, of Water Molecules around F^-, K^+ and of F^- around K^+ in Aqueous KF Solution as a Function of Molality (KF mol/kg of water)

system	1	2	3	4	5	6
molality	2.84	3.70	5.56	9.26	10.72	14.40
τ_{Fw}	25	26	30	32	40	43
τ^1_{Kw}	11	12	21	33	32	52
τ^2_{Kw}	11	12	14	19	20	26
τ_{KF}	72	70	77	90	75	97

which the enclosed peak does not appears. We will speak of τ^1_{Kw} for the first case and of τ^2_{Kw} for the second. Then the function $P_{ij}(t, t_0;t^*)$ is introduced, its values can be either equal to 0 or 1. It takes the value 1 if the distance at both times t_0 and $(t + t_0)$ is smaller than r_{cut}, and if in this interval it does not exceed such a value for any period longer than t^*. Otherwise, it takes the value 0. The parameter t^* allows the water molecule to temporarily leave the vicinity of ions, while still being considered as solvated. In other words, it amounts to assuming that the width of the solvation shell is not strictly equal to r_{cut} but may fluctuate around this value. In agreement with others authors,[3,8] we have taken t^* equal to 2 ps, the characteristic residence time of a water molecule in pure water. Then we define $n(t)$ as the average number of water molecules, solvated at time t_0 by an ion, and still solvated after a time t. It is defined as

$$n(t) = \frac{1}{t_{corr}} \frac{1}{N_i} \sum_{t_0=1}^{t_{corr}-t} \sum_{i=1}^{N_i} \sum_{j=1}^{N_j} P_{ij}(t,t_0;t^*) \qquad (4)$$

where N_i is the number of solvated ions, N_j is the number of solvating water molecules, t_{corr} the total correlation time, i.e., here the length of the simulated trajectory. It follows immediately from eq 4 that $n(0)$ is the average coordination number of water molecules around the ions. The residence time τ of water molecules in the vicinity of ions is then calculated as the characteristic relaxation time for $n(t)$, assuming that, except at short times, $n(t)$ has an exponential decay:

$$n(t) = n(0) \exp(-t/\tau) \qquad (5)$$

Using the same definitions, we have calculated the residence times of F^- around K^+, taking N_i as the number of K^+ and N_j as the number of F^-, while keeping t^* equal to 2 ps. For all calculations the correlation time, t_{corr}, was equal to 204 ps. The resulting errors are of 10%.

As expected, residence times of water around ions increase as C_{KF} grows, in agreement with the finding of the decline of the diffusion coefficients D_K and D_F with C_{KF} for both ions. As C_{KF} grows, the various species loose some degrees of freedom and are less and less moving. Accordingly, there are less and less exchanges between the solvation shells and the bulk.

The two different definitions for the residence time of water molecules around K^+ ions give notably different results. The times calculated for the "first hydration shell", τ^2_{Kw}, are smaller than those taking into account also the enclosed peak, τ^1_{Kw}. This is not surprising considering that the distance cutoff in the case of τ^1_{Kw} is greater than τ^2_{Kw}: the exchanges between the coordination spheres and the bulk are less frequent. But at the highest C_{KF}, knowing that the difference between both distance cutoff is only 1 Å, the ratio of 2 between both residence times appears significant, and supports the existence of a well-defined second hydration shell for the ion.

Whatever C_{KF} is, τ_{Fw} is always greater than τ^2_{Kw}, most probably as a result of the strong hydrogen-bond created between F^- and the water molecules. Interactions between water molecules and F^- are then more attractive than in the case of K^+, and exchanges of water molecules are less frequent. This is still the case when comparing to τ^1_{Kw} except for the highest concentration, a change probably due to the increasing stability of the outer shell of solvation for K^+, whose contribution becomes more pronounced than at smaller concentrations.

Finally, the residence times τ_{KF} are far longer than all others. We may once more conclude that ion pairing is a very stable feature in the concentrated solutions we have studied.

VI. Discussion

For each solution, whatever C_{KF} is, the first coordination shell of each species in solution is respected, while compared to infinitely diluted solutions and pure water. But afterward, it is not anymore the case, especially for the K^+−water and water−water interactions: in both cases, studying the corresponding $g_{ij}(r)$, an enclosed peak appears in the first one. Concerning the $g_{KO}(r)$, it is interesting to notice that the enclosed KO peak appears at the usual first minimum distance calculated in simulations with a single K^+ in water.[13] For a comparison, consider the ab initio calculations of Lee et al.,[51] where it has been found that the most energetically stable $K^+(H_2O)_6$ cluster in the gas phase has a $4+2(C_2)$ structure: with four water molecules in an inner shell (i) and two water molecules, hydrogen-bonded to the first ones, in an outer shell (o). The related distances are $r^i_{KO} = 2.65$ and 2.87 Å, $r^o_{KO} = 3.75$ Å. Those distances are close to the positions of the peaks in the radial distribution functions and, though they have been calculated in the gas phase, they can be taken as reference distances for configurational studies.

Finally, a solvation geometry takes the place of the usual hydrogen-bond pattern of water, decreasing but still allowing a large number of water dimers to form hydrogen-bonds between them. The combined study of the $g_{OO}(r)$ and of the water−water dimerization energies demonstrates this point: the probability of water−water hydrogen-bonding decreases as C_{KF} grows, but is still relevant at very high concentrations. On the other hand, the tetrahedral structure of water is lost.

Looking now at both the $g_{ij}(r)$ and the dynamical properties of ions, one can postulate the existence of long living ionic pairs at all concentrations. A study of the conductivity may be interesting in order to analyze this fact, but unfortunately experimental data are missing at such concentrations. Even so, we should better speak, for our systems, of a solvation of KF pairs in solutions. These features partially explain the difficulties in fully describing the ion solvation structures, using the $g_{ij}(r)$ ion−water only. The solvation structures of K^+ and F^- interact directly, and modify one another. The fact that the calculated $2n_{KO} \neq n_{KH}$ is often interpreted in terms of a less defined first shell around K^+ compared to smaller ions, as Li^+ or Na^+, and then important exchanges of water molecules may falsify accurate calculations.[3,13] In our case, the cooperative solvation effect may explain too this great difference (at 5.16 mol/L, $2n_{KO} = 12.5$, compared to $n_{KH} = 22.7$).

If we compare now the differences between Potential 1 and Potential 2, it is interesting to notice that the little change of the σ_{OF} parameter induced great changes for macroscopic quantities and also for microscopic features. In Table 6, we have given the water−ion structural features for Potential 1 for the

5.16 mol/L system. The water−fluoride distances are different, that is an immediate consequence of the change of parameter, but also the water−ions coordination numbers are different. It can be seen that the coordination numbers of water molecules around ions, using Potential 1, are close to those calculated in the infinite dilution limit. On the other hand, the KF coordination number equals 0.4 for Potential 1, which is very low compared to the 1.4 calculated for Potential 2. The encapsulated graph of Figure 7 gives the water−fluoride pair interaction energies for both potentials. The maxima of both potentials are the same, but it is obvious that the probability at this point is far greater for Potential 1 than for Potential 2. The residence time of water molecules around the potassium ions is quite the same for both potentials, and it is a bit greater around the fluoride ions for Potential 1 (44 compared to 30 ps). But the ion−ion residence time is different: 35 ps using Potential 1, compared to 77 ps using Potential 2 It is then obvious that the change in the model potential induced a significant change in the microscopic description of our system: the water−F^- interactions are lowered, and the ion solvation observed using Potential 1 is replaced by the pairing solvation mentioned above.

VII. Conclusion

We have performed MD simulations of KF aqueous solutions up to very high concentrations, from 2.8 M up to 11.9 M, at $T = 298$ K on the basis of a new interaction model we propose here to resolve the inadequacy of the potential parameters taken from the literature, which fail to reproduce satisfactorily two basic experimental properties such as the solution density and water self-diffusion coefficients. The new model results from a small change to the a priori weakest part, i.e., the water−ion interaction potential which is inferred from gas-phase ab initio calculations, while the model for water (SPC/E) and for ion−ion interactions (Tosi/Fumi) are kept fixed. A microscopic description of the solutions as a function of concentration has been given in terms of partial distribution functions and of pair energy distributions and dynamical properties such as self-diffusion coefficients and residence times.

Our main results are that the hydrogen-bonded structure of water is substituted by the solvation structure as the salt concentration grows and that a strong tendency is found for K^+-F^- ion pairing, stable at long times.

At this point, it may be interesting to study further and more deeply the different features of the solutions at a microscopic level with more sophisticated analysis tools. However we feel that the lack of accurate experimental structural data to compare with our findings makes this route not so interesting because the validity of the model relies on a comparison with experiment which, despite the very good agreement as a function of concentration, is severely limited to just two properties, density and water self-diffusion. On the contrary, a more sound microscopic structure to compare with can nowadays be obtained by accurate ab initio calculations and it can serve as an alternative starting point to develop systematically more accurate effective potential models to be used in large-scale simulations. Work is in progress in this direction using the first principles molecular dynamics with density functional approach of Car and Parrinello.[55]

References and Notes

(1) Clementi, E.; Barsotti, R.; Fromm, J.; Watts, R. O. *Theor. Chim. Acta (Berlin)* **1976**, *43*, 101.
(2) Watts, R. O. *Mol. Phys.* **1976**, *32*, 659.
(3) Impey, R. W.; Madden, P. A.; McDonald, I. R. *J. Phys. Chem.* **1983**, *87*, 5071.
(4) Bounds, D. G. *Mol. Phys.* **1985**, *54*, 1335.
(5) Guàrdia, E.; Rey, R.; Padró, J. A. *J. Chem. Phys.* **1991**, *95*, 2823.
(6) Dang, L. X.; Smith, D. E. *J. Chem. Phys.* **1993**, *99*, 6950.
(7) Lee, S. H.; Rasaiah, J. C. *J. Chem. Phys.* **1994**, *101*, 6964.
(8) Lyubartsev, A. P.; Laaksonen, A. *J. Phys. Chem.* **1996**, *100*, 16410.
(9) Lee, S. H.; Rasaiah, J. C. *J. Phys. Chem.* **1996**, *100*, 1420.
(10) Periole, X.; Allouche, D.; Daudey, J.-P.; Sanejouand, Y. H. *J. Phys. Chem. B*, **1997**, *101*, 5018.
(11) Koneshan, S.; Rasaiah, J. C.; Lynden-Bell, R. M.; Lee, S. H. *J. Phys. Chem. B* **1998**, *102*, 4193.
(12) Tongraar, A.; Liedl, K. R.; Rode, B. M. *J. Phys. Chem. A* **1998**, *102*, 10340.
(13) Ramaniah, L. M.; Bernasconi, M.; Parrinello, M. *J. Chem. Phys.* **1999**, *111*, 1587.
(14) Lee, S. H.; Cummings, P. T. *J. Chem. Phys.* **2000**, *112*, 864.
(15) Jorgensen, W. L.; Chandrsekhar, J.; Madura, J. D.; Impey, R. W.; Klein, M. L. *J. Chem. Phys.* **1983**, *79*, 926.
(16) van der Spoel, D.; van Maaren, P. J.; Berendsen, H. J. C. *J. Chem. Phys.* **1998**, *108*, 10220.
(17) Jedlovszky, P.; Richardi, J. *J. Chem. Phys.* **1999**, *110*, 8019.
(18) Fumi, F. G.; Tosi, M. P. *J. Phys. Chem. Solids* **1964**, *25*, 31.
(19) Tosi, M. P.; Fumi, F. G. *J. Phys. Chem. Solids* **1964**, *25*, 45.
(20) Lewis, J. W. E.; Singer, K.; Woodcock, L. V. *J. Chem. Soc., Faraday Trans. 2* **1975**, *71*, 301.
(21) Hansen, J.-P.; McDonald, I. R. *Theorie of simple liquids*, 2nd ed.; Academic Press: London, 1986.
(22) Pettitt, B. M.; Rossky, P. J. *J. Chem Phys.* **1986**, *84*, 5836.
(23) Zhu, S.-B.; Robinson, G. W. *J. Chem. Phys.* **1992**, *97*, 4336.
(24) Degrève, L.; da Silva, F. L. B. *J. Chem. Phys.* **1999**, *110*, 3070.
(25) Hawlicka, E.; Swiatla-Wojcik, D. *Phys. Chem. Chem. Phys.* **2000**, *2*, 3175.
(26) Berendsen, H. J. C.; Postma, J. P. M.; von Gunsteren, W. F.; Hermans, J. *Intermolecular Forces*; B. Pullman: (Reidel, Dordrecht), 1981; pp 331−342.
(27) Berendsen, H. J. C.; Grigera, J. R.; Straatsma, T. P. *J. Phys. Chem.* **1987**, *91*, 6269.
(28) Dang, L. X. *Chem. Phys. Lett.* **1992**, *200*, 21.
(29) Dang, L. X. *J. Am. Chem. Soc.* **1995**, *117*, 6954.
(30) Allen, M. P.; Tildesley, D. J. *Computer Simulation of Liquids*; Oxford University Press: Oxford, 1987.
(31) Ewald, P. *Ann. Phys.* **1921**, *64*, 253.
(32) Ciccotti, G.; Ferrario, M.; Ryckaert, J.-P. *Mol. Phys.* **1982**, *47*, 1253.
(33) Ryckaert, J.-P.; Ciccotti, G.; Berendsen, H. J.-C. *J. Comput. Phys.* **1977**, *23*, 327.
(34) Ciccotti, G.; Ferrario, M.; Ryckaert, J.-P. *Mol. Phys.* **1982**, *47*, 1253.
(35) Nosé, S. *Mol. Phys.* **1984**, *52*, 255.
(36) Nosé, S. *J. Chem. Phys.* **1984**, *81*, 511.
(37) Hoover, W. G. *Phys. Rev. A* **1985**, *31*, 1695.
(38) Nosé, S. *Prog. Theor. Phys.* **1991**, *103*, 1.
(39) Andersen, H. C. *J. Chem. Phys.* **1980**, *72*, 2384.
(40) Ferrario, M.; Ryckaert, J. P. *Mol. Phys.* **1985**, *54*, 587.
(41) Lobo, V. M. M.; Quaresma, J. L. *Electrolyte solutions: Literature data on thermodynamic and transport properties*; D. de Quimica da Universidade de Coimbra, 1984.
(42) Müller, K. J.; Hertz, H. G. *J. Phys. Chem.* **1996**, *100*, 1256.
(43) Klopper, W.; van Duijneveldt-van de Rijdt, J. G. C. M.; van Duijneveldt, F. B. *Phys. Chem. Chem. Phys.* **2000**, *2*, 2227.
(44) Starr, F. W.; Nielsen, J. K.; Stanley, H. E. *Phys. Rev. E* **2000**, *62*, 579.
(45) Medeiros, M.; Costas, M. E. *J. Chem. Phys.* **1997**, *61*, 2012.
(46) Soper, A. K.; Bruni, F.; Ricci, M. A. *J. Chem. Phys.* **1997**, *106*, 247.
(47) Stillinger, F. H.; Rahman, A. *J. Chem. Phys.* **1974**, *60*, 1545.
(48) Stillinger, F. H.; Rahman, A. *J. Chem. Phys.* **1974**, *61*, 4973.
(49) Chialvo, A. A.; Cummings, P. T. *J. Phys. Chem.* **1996**, *100*, 1309.
(50) Ferrario, M.; Tani, A. *Chem. Phys. Lett.* **1985**, *121*, 182.
(51) Lee, H. M.; Kim, J.; Lee, S.; Mhin, B. J.; Kim, K. S. *J. Chem. Phys.* **1999**, *111*, 3995.
(52) Newsome, J. R.; Neilson, G. W.; Enderby, J. E. *J. Phys. Chem.* **1980**, *13*, 923.
(53) Degrève, L.; de Pauli, V. M.; Duarte, M. A. *J. Chem. Phys.* **1997**, *106*, 655.
(54) Bryce, R. A.; Vincent, M. A.; Malcolm, N. O. J.; Hillier, I. H.; Burton, N. A. *J. Chem. Phys.* **1998**, *109*, 3077.
(55) Car, R.; Parrinello, M. *Phys. Rev. Lett.* **1985**, *55*, 2471.